

CHLORITOID INCLUSIONS IN PYRITE FROM NAVAJÚN, SPAIN

KATHARINA LODDERS¹

*Planetary Chemistry Laboratory, Department of Earth and Planetary Sciences, Washington University,
Campus Box 1169, St. Louis, Missouri 63130-4899, U.S.A.*

GÖSTAR KLINGELHÖFER

Institut für Kernphysik, Technische Universität Darmstadt, Schloßgartenstrasse 9, D-64289 Darmstadt, Germany

DANIEL T. KREMSER

*Department of Earth and Planetary Sciences, Washington University, Campus Box 1169, St. Louis,
Missouri 63130-4899, U.S.A.*

ABSTRACT

Almost pure Fe end-member chloritoid was identified as the major included phase in large cubes of pyrite from Navajún, Logroño, Spain. The silicates in the pyrite matrix as well as isolated mineral separates were analyzed by electron microprobe, X-ray diffraction, and Mössbauer spectroscopy. Mössbauer spectra taken at room temperature and at 77 Kelvin show a superposition of an Fe²⁺ doublet and at least one Fe³⁺ doublet. The chloritoid from one of the pyrite cubes analyzed is more oxidized than that in the two other cubes. Mössbauer data give some evidence that this may be due to the presence of Fe³⁺ in sites normally occupied by Fe²⁺. In all samples, significant effects due to preferred orientation have been observed in both the X-ray and Mössbauer spectra.

Keywords: chloritoid, pyrite, Mössbauer spectroscopy, Navajún, Logroño, Spain.

SOMMAIRE

Nous avons identifié la chloritoïde, de composition proche du pôle (ferrique), comme inclusion principale dans les cubes de pyrite provenant de Navajún, Logroño, en Espagne. Les silicates présents dans la matrice de ces cubes ainsi que des concentrés isolés ont été analysés avec une microsonde électronique, et par diffraction X et spectroscopie de Mössbauer. Les spectres de Mössbauer, prélevés à température ambiante et à 77 K, montrent une superposition d'un doublet attribué au Fe²⁺ et d'au moins un doublet attribué au Fe³⁺. La chloritoïde d'un des cubes de pyrite analysés possède plus de Fe³⁺ que celle des deux autres. Les données de Mössbauer font penser qu'il s'agit de Fe³⁺ normalement situé dans les sites du Fe²⁺. Dans tous les échantillons, les effets d'une orientation préférentielle ont été repérés dans les spectres de diffraction X et de Mössbauer.

(Traduit par la Rédaction)

Mots-clés: chloritoïde, pyrite, spectroscopie de Mössbauer, Navajún, Logroño, Espagne.

INTRODUCTION

We investigated the purity of pyrite samples from different localities in order to find suitable material to experimentally study the kinetics of pyrite decomposition on Venus (Fegley *et al.* 1995). We found that the large and strikingly euhedral cubes of pyrite from Navajún, Logroño, Spain, contain chloritoid, of general formula (Fe²⁺,Mg,Mn)₂(Al,Fe³⁺)(OH)₄Al₃O₂[SiO₄]₂, as an important silicate inclusion. Chloritoid has been

reported in over a hundred localities and in several different types of geological settings, as described by Halferdahl (1961). Chloritoid is a common metamorphic mineral in pelitic rocks, and is used as an index mineral of metamorphism; see Vidal *et al.* (1994) and references therein for a recent overview and studies on the stability of chloritoid. The occurrence of chloritoid in pyrite has not yet been reported, although Gustafson (1946) noted the occurrence of chloritoid in the Hollinger mine, Porcupine district, Ontario, where the walls of hydro-

¹ E-mail address: lodders@levee.wustl.edu

thermal gold–quartz veins are strongly pyritized. The chloritoid at the Hollinger locality is commonly concentrated about pyrite and tourmaline, which were both introduced *via* a hydrothermal fluid; Gustafson (1946) thus regarded chloritoid as a product of hydrothermal alteration.

The Soria and La Rioja provinces (formerly Logroño), Spain, are probably the best known localities for large, idiomorphic crystals of pyrite, which can reach up to 20 cm length on a side (Calvo & Sevillano 1989). According to these authors, the pyrite is found in hard marl, which is composed of more than 50% clay and at least 15% calcium carbonate. Very little else is known about the host rock of the pyrite. Furthermore, there is no mention of silicate inclusions in the pyrite. Here, we report the results of our electron microprobe, X-ray diffraction, and Mössbauer studies of the chloritoid inclusions in these crystals of pyrite.

EXPERIMENTAL PROCEDURES

Samples and sample preparation

Pyrite cubes from Navajun, Spain were obtained from Ward's Scientific, Rochester, New York. Three cubes (about 2.5 cm on a side) were investigated in detail, and were designated NLS0, NLS5, and NLS7. The outside faces of the pyrite cubes display smooth surfaces, with no visible inclusions. The density of the pyrite (determined by weighing and measuring the lengths of the axes of the cubes) is about 4.75 g/cm³, lower than the tabulated values of 4.99–5.03 g/cm³ (Deer *et al.* 1966), suggesting the presence of less dense phases. The pyrite cubes are free of host material, which was obtained separately and analyzed.

The cubes were cut into slices about 1 mm thick; these were polished to a 0.25 µm finish. The interior of the cubes show abundant inclusions under the microscope (Fig. 1). In order to isolate the inclusions for analysis, large chunks of the pyrite cubes were dissolved in nitric acid and subsequently in aqua regia at room temperature, which gave either a dark green residue or a more fine-grained yellow residue. The green, coarse residues were obtained from samples with abundant inclusions, easily visible without a microscope. Once isolated, the inclusions were cleaned with distilled water and acetone. The procedure of chemical isolation removed carbonates and sulfates typically present in minor amounts in the pyrite. X-ray-diffraction patterns and electron-microprobe analyses of chloritoid obtained from untreated chloritoid-bearing pyrite and the residue samples after pyrite dissolution are similar, and suggest that this procedure did not alter the chemical composition of the chloritoid. Unfortunately, *in situ* Mössbauer spectroscopy of chloritoid inclusions in pyrite, which could confirm that chloritoid is unaffected during isolation, is very difficult because of the low abundance

of chloritoid in the pyrite samples and the strong signals from the iron in the pyrite matrix.

Electron-microprobe analyses

Electron-microprobe analyses were done on the small inclusions of chloritoid in the pyrite matrix (Fig. 2) as well as on isolated grains that were mounted in epoxy. The latter were analyzed for comparison to

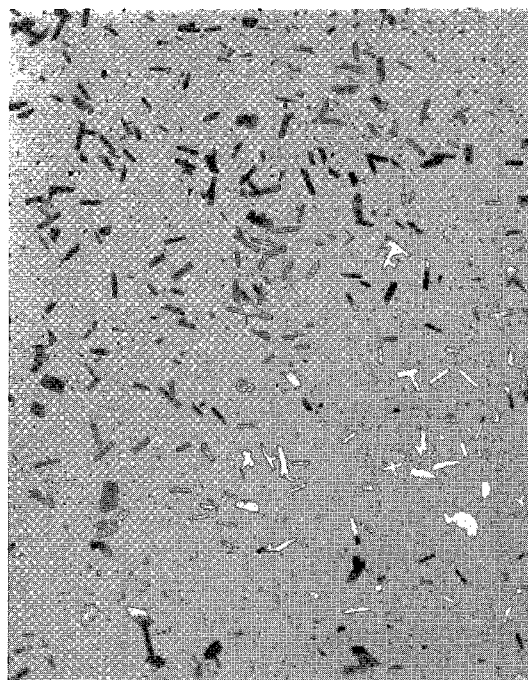


FIG. 1. Inclusions in pyrite from Navajun, Spain. Whereas the outer surfaces of the cubes are free of inclusions, the interior is filled with randomly oriented needles of chloritoid. The field of view is 2.25 mm.

in situ chloritoid to evaluate whether any excess iron signals arose owing to the pyrite matrix. Microprobe analyses were done on the Washington University JEOL 733 electron microprobe equipped with Advanced MicroBeam Incorporated automation. For the analyses, an accelerating voltage of 15 kV and a beam current of 15 nA was employed. In most cases, a beam spot 5 µm in diameter was used. X-ray matrix corrections were based on a modified CITZAF routine (Armstrong 1988) incorporated in the software. X rays for Si, Al, Fe, Mn, Mg, and Ti were counted. No other elements (above atomic number 9 and >0.02 wt%) were detected in wavelength scans. This is also confirmed by INAA analyses (see Table 1). The proportion of oxygen was calculated by cation stoichiometry and included in the matrix correction.

TABLE 1. INAA DATA FOR PYRITE FROM NAVAJUN, SPAIN, AND ISOLATED INCLUSIONS

	Pyrite (NLS5)		Silicate Inclusions (NLS0)	
Fe	45.43%	(3)	19.00%	(3)
Na	54	(3)	840	(3)
K	175	(3)	1900	(3)
Sc	1.7	(4)	32.1	(3)
Cr	37	(4)	310	(3)
Mn	43	(3)	1215	(3)
Co	73	(3)	10	(10)
Ni	640	(10)	96	(25)
Zn	18	(10)	610	(4)
Ga	1.6	(10)	54	(3)
As	2.5	(3)	1.8	(4)
Zr	120	(15)	470	(15)
Sb	1.6	(3)	5.9	(4)
La	14.7	(3)	39.9	(3)
Ce	29.7	(5)	96.4	(4)
Pr	3.1	(7)	11	(12)
Nd	10.6	(7)	43	(10)
Sm	2.49	(5)	11.6	(3)
Eu	0.548	(3)	3.35	(3)
Tb	0.41	(10)	1.55	(4)
Dy	2.3	(5)	9.0	(4)
Ho	0.54	(10)	1.96	(4)
Er	1.5	(15)	5.7	(20)
Yb	1.63	(4)	5.53	(4)
Lu	0.26	(4)	0.83	(5)
Hf	3.2	(4)	11.2	(4)
Ta	0.9	(4)	2.5	(5)
W	2.9	(4)	7.0	(4)
Au	0.053	(3)	<0.005	
Th	9.14	(3)	16.4	(4)
U	2.39	(4)	5.42	(3)

Data in ppm except Fe in wt%. Parenthesis show uncertainty from counting statistics in %. Analyses are courtesy of B. Spettel, MPI Mainz, Germany.

X-ray-diffraction analysis

The X-ray-diffraction patterns were obtained using a RIGAKU vertical powder diffractometer with $\text{CuK}\alpha$ radiation ($\lambda = 1.540598 \text{ \AA}$) and Material Data Incorporated software. The samples of chloritoid residue were finely ground, mixed with an internal standard (NIST

640b silicon) and placed on standard glass X-ray slides. Each sample was scanned from 10 to $70^\circ 2\theta$ with a step size of $0.02^\circ 2\theta$ and a dwell time per step of one second.

Mössbauer spectroscopy

The isolated samples were analyzed at different temperatures by ^{57}Fe -Mössbauer spectroscopy using a loudspeaker-type drive in constant acceleration mode and a triangular velocity-reference signal. ^{57}Co sources in a Rh matrix, with activities between about 40 mCi and 150 mCi, were used for the measurements. A Si-PIN-diode was used as gamma-ray detector for room-temperature measurements (Klingelhöfer *et al.* 1995), whereas a bath-type cryostat in combination with a proportional counter (Ar-CH_4 gas mixture) was employed for low-temperature measurements. The linearity in velocity of the drive systems is better than about 0.1%, so that no corrections are needed for data analysis. The spectrometers were calibrated for each run using a standard α -Fe metal foil. The source was kept at room temperature for the low-temperature measurements. The center shift of the different components, which corresponds to the isomer shift at 0 K and otherwise includes the second-order Doppler shift value, is given relative to α -Fe at room temperature and is abbreviated in all cases as IS.

The sample thickness was chosen to be equivalent to less than 4 mg Fe/cm^2 , so that thickness effects can be considered to be small. Most of the measurements were done on samples of chloritoid residue as obtained after the isolation procedure described above. To check the influence of preferred orientation, some samples were ground to a fine powder and analyzed at different angles of incidence between the γ rays and sample. The Mössbauer parameters were determined by a least-squares fitting routine developed in Darmstadt, Germany. Lorentzian or Voigt line-shapes were assumed for the two doublets, which were found to be sufficient to obtain a good fit for all data. No statistically significant improvement of the fit was achieved by using more than two doublets.

RESULTS AND DISCUSSION

Minerals in pyrite

The outer faces of the pyrite cubes are normally free of inclusions, which appear randomly oriented in the interior of the cubes (Fig. 1). The major included phase is chloritoid, which occurs as needles up to $100 \mu\text{m}$ long and $20\text{--}60 \mu\text{m}$ wide. The X-ray-diffraction analyses on powdered samples of pyrite and on the residues after dissolution led to the initial detection of chloritoid. Pyrite was not detected in the samples of residue; in addition to chloritoid, rutile, quartz, muscovite, and possibly clinocllore were identified by X-ray diffraction.

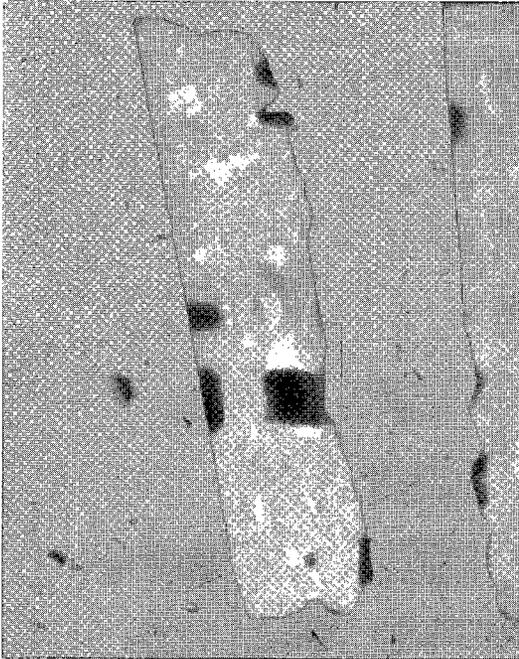


FIG. 2. Typical inclusions of chloritoid in pyrite matrix, shown in a back-scattered electron image. Chloritoid itself commonly contains inclusions of rutile (bright areas), and occasionally quartz inclusions are also observed (dark). The field of view is 90 μm .

The presence of these phases was confirmed by electron microscopy. Other matrix minerals identified by energy-dispersion spectrometry (EDS) are calcite, anhydrite, zircon and a light-rare-earth-rich phosphate. Quartz and rutile were observed within the chloritoid needles, but ilmenite, which also is known to occur within chloritoid (Halferdahl 1961, Tricker *et al.* 1978), was not found here.

Results of representative instrumental neutron-activation analyses (kindly provided by B. Spettel, MPI Mainz, Germany) of a bulk sample of pyrite and of the isolated mineral inclusions are given in Table 1. A comparison of the iron content of pure pyrite (46.55%) with the iron content of the bulk pyrite sample gave 2.4 wt% inclusions in pyrite. A gravimetric determination by combustion of pyrite in air indicated that about 3 wt% of inclusions are present. The presence of inclusions containing rare-earth elements (*REE*) in quantities detectable by the electron microprobe is compatible with the relatively high concentrations of the *REE* in bulk pyrite and in isolated samples of inclusions analyzed by instrumental neutron activation. In bulk pyrite samples, the total concentration of *REE* amounts to ~70–90 ppm, and U and Th concentrations are 2.5 ppm and 7–9 ppm, respectively. Zirconium in bulk

pyrite is about 120 ppm, which is consistent with minor amounts of observed zircon. The amount of iron (19 wt%) in the bulk silicate inclusion sample is comparable to the amount of total iron in chloritoid (~20 wt%) analyzed by electron microprobe, in agreement with our finding that chloritoid is the major silicate inclusion present.

In all mineral separates, only triclinic chloritoid was identified by X-ray diffraction, and monoclinic chloritoid appears to be absent. Calculation of a least-squares fit of the chloritoid cell constants (using *d*-values) proved unsuccessful owing to the multiple overlaps of lines originating from the other phases present in the residues and the discrepancies in relative intensity. The line intensities of chloritoid are strongly affected by grain size and ordering effects. Diffraction patterns taken from bulk pyrite powders and the residues needed careful grinding and sample mounting to avoid a strong dominance of the 4.44 Å reflection. For example, patterns of differently prepared samples of the yellow residue from NLS5 were taken under otherwise constant conditions. The diffraction pattern of the powdered fine residue as obtained from the chemical isolation procedure was dominated by the very intense 4.44 and 2.96 Å reflections from the 002 and 003 planes. The same material crushed dry showed decreases in intensities of these reflections, and other reflections became visible, but relative intensity-ratios were still different than those reported in the literature (Halferdahl 1961). After further grinding this sample in acetone and dispersing the very fine powder with acetone on the sample holder, all of the characteristic *d*-values for chloritoid were visible, and relative intensities were much closer to values reported in the literature.

Chemical composition of chloritoid from electron-microprobe analyses

Table 2 shows the composition of chloritoid from results of the electron-microprobe analyses, and, for comparison, data for Fe-rich chloritoid by Chopin *et al.* (1992) and for ideal pure Fe-end-member chloritoid. The chloritoid commonly contains small (~6 μm) inclusions of rutile, which appear as bright spots in back-scattered electron images, and dark-gray-appearing quartz (Fig. 2). Both minerals are known to be associated with chloritoid. Halferdahl (1961) noted that Ti may enter the structure, but that the maximum amount in chloritoid is probably less than 0.6% TiO_2 . Therefore, compositions with a high TiO_2 content are likely due to minuscule inclusions of rutile. Ilmenite also has been reported as an impurity in chloritoid, but was not detected during electron-microprobe analyses or by Mössbauer spectroscopy. Chloritoid compositions commonly are corrected for rutile and ilmenite content (Tricker *et al.* 1978, Halferdahl 1961). Corrections for quartz in chloritoid have also been reported. We

TABLE 2. ELECTRON MICROPROBE DATA (wt%) FOR CHLORITOID IN PYRITE FROM NAVAJUN, SPAIN

	NLS-0 in pyrite	NLS-0 residue	NLS5 in pyrite	NLS5 green residue	NLS5 yellow residue	NLS7 in pyrite	NLS7 residue	in Host Rock	Chopin <i>et al.</i> 1992 ^c	Ideal Chloritoid
SiO ₂	23.8±0.2	24.0±0.1	23.9±0.1	24.0±0.1	23.8±0.2	24.2±0.1	24.0±0.3	24.5±0.2	23.70	23.85
Al ₂ O ₃	41.0±0.4	40.9±0.5	40.4±0.9	40.7±0.5	40.7±0.2	40.8±0.3	40.9±0.4	41.3±0.3	39.71	40.48
Fe ₂ O ₃ *	1.72±0.04	1.76±0.02	6.33±0.06	6.37±0.13	6.23±0.09	2.32±0.03	2.27±0.03	5.65±0.11	0.66	0
FeO*	24.2±0.5	24.4±0.2	20.2±0.2	20.3±0.4	19.9±0.3	24.0±0.3	23.5±0.3	20.4±0.4	26.43	28.52
MnO	0.22±0.04	0.27±0.04	0.27±0.02	0.27±0.04	0.28±0.02	0.28±0.06	0.28±0.01	0.40±0.02	0.20	0
MgO	0.98±0.20	0.95±0.14	0.88±0.06	0.91±0.20	0.86±0.13	0.92±0.13	0.90±0.08	1.10±0.11	0.90	0
TiO ₂ ^a	<0.2	<0.3	<0.02	<0.09	<0.3	<0.12	<0.3	<0.02	0.01	0
TOTAL	91.9±0.7	92.3±0.6	92.0±0.9	92.6±0.7	91.8±0.5	92.5±0.5	91.8±0.6	93.3±0.6	91.77	92.85
H ₂ O ^b	8.1	7.7	8.0	7.4	8.2	7.5	8.2	6.7	8.23	7.15
Atomic Proportions (Si = 2.0)										
Si	(2.00)	(2.00)	(2.00)	(2.00)	(2.00)	(2.00)	(2.00)	(2.00)	(2.00)	(2.00)
Al	4.06	4.02	3.98	4.00	4.02	3.97	4.02	3.97	3.95	4
Fe ³⁺	0.11	0.11	0.40	0.40	0.39	0.14	0.14	0.35	0.042	0
Fe ²⁺	1.70	1.70	1.41	1.41	1.39	1.65	1.64	1.39	1.865	2
Mn	0.016	0.019	0.019	0.019	0.020	0.020	0.020	0.028	0.014	0
Mg	0.12	0.12	0.12	0.11	0.11	0.11	0.11	0.13	0.11	0
OH	4.52	4.32	4.44	4.15	4.61	4.12	4.36	3.65	4.64	4
Al + Fe ³⁺	4.17	4.13	4.38	4.40	4.41	4.11	4.16	4.32	3.99	4
Fe ²⁺ +Mn+Mg	1.84	1.84	1.55	1.54	1.52	1.78	1.77	1.55	1.99	2
M ²⁺ + M ³⁺	6.01	5.97	5.93	5.94	5.93	5.90	5.93	5.87	5.98	6

±: 1 σ deviation of multiple (5-10) spot analyses.

* Amount of Fe₂O₃ and FeO calculated from the total amount of Fe determined by electron probe and the Fe²⁺/Fe³⁺ ratio determined from Mössbauer spectroscopy. The stated uncertainties are derived by scaling the 1 σ deviations from the electron probe data for total Fe.

a: Only analyses with TiO₂ content < 0.5 wt% were considered.

b: By difference from 100%.

c: Analysis no. 11 of Table 3 by Chopin *et al.* (1992). They assume $|4-M^{3+}| = 2|2-M^{2+}|$ to calculate the Fe²⁺/Fe³⁺ ratio. The total includes (in wt%) Cr₂O₃ (0.02), ZnO (0.06), BaO (0.03), CaO (0.01), K₂O (0.01), F (0.03).

avoided analyses of chloritoid in direct vicinity of rutile or quartz inclusions, and only considered compositions with less than 0.5% TiO₂. We also analyzed for Ca; in most cases, Ca was found to be absent. Similarly, Na and K are present only in very small amounts, as also indicated by the INA analyses. No other elements above atomic number nine were detected in wavelength scans.

The amount of iron as Fe₂O₃ listed in Table 2 was calculated from the total Fe determined by electron microprobe and the Fe²⁺/Fe³⁺ ratio derived from the Mössbauer data (see below). The amount of H₂O was then obtained by difference from 100%. The calculated H₂O contents of the chloritoid samples are higher than those expected from ideal stoichiometry, but within uncertainties fall into the expected range of values for

most samples. In Table 2, we also compare our data to a composition of Fe-rich chloritoid reported by Chopin *et al.* (1992). Apparently, the analytical totals indicate higher H₂O abundances in chloritoid than expected from the ideal formula, as is also seen from the composition of several samples reported by Chopin *et al.* (1992).

Compositions of the chloritoid in the pyrite matrix and of isolated grains in an individual cube of pyrite are very similar, and suggest that the isolation procedure apparently did not alter the chloritoid's composition. The chloritoid is very Fe-rich; Mg plus Mn are present in small amounts only (<1.5% MgO + MnO). The amount of Al is very close to the concentration expected for ideal chloritoid, so the amount of Fe³⁺ in the samples must be relatively low. However,

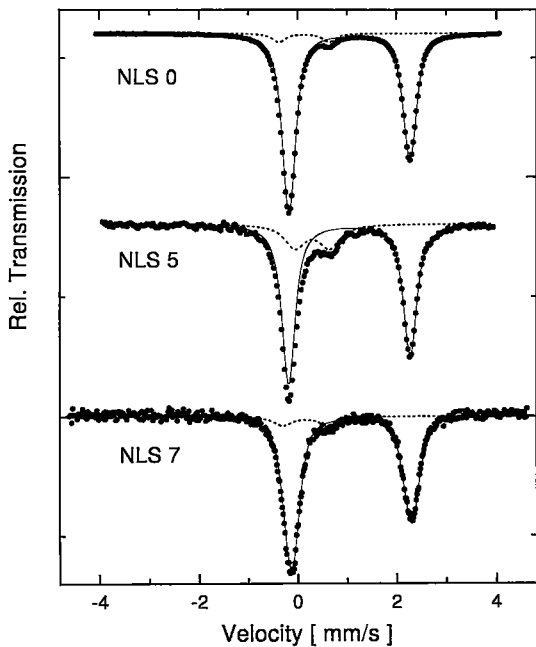


FIG. 3a. Mössbauer spectra of samples NLS0, NLS5, and NLS7. Spectra are taken at room temperature. The full line corresponds to the Fe^{2+} component, and the dotted line, to Fe^{3+} .

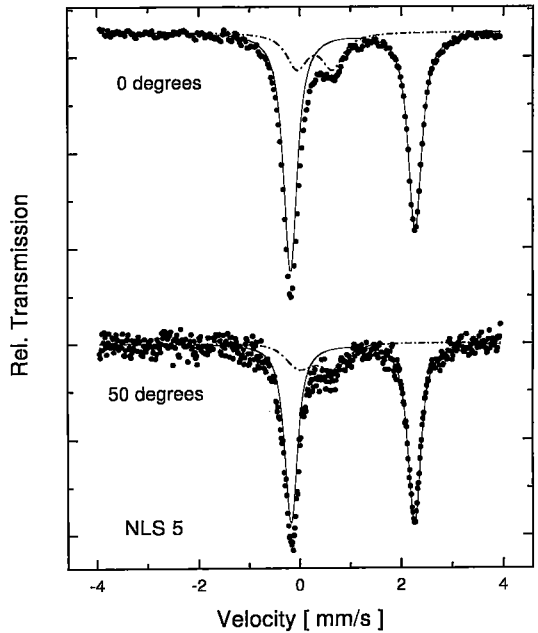


FIG. 3b. Mössbauer spectra of a sample of residue NLS5 taken at two different angles of incidence. Spectra are taken at room temperature. The full line corresponds to the Fe^{2+} component, the dotted line, to Fe^{3+} , respectively.

Mössbauer spectroscopy shows that $\text{Fe}^{3+}/\text{Fe}^{2+}$ values are higher than expected from the ideal formula.

The Mössbauer spectra of various samples from the NLS5 chloritoid clearly show that the Fe^{3+} component is stronger than in chloritoid from NLS0 and NLS7. The percentage of total Fe present as Fe^{3+} in chloritoid from NLS5 is about 22%, whereas the respective percentages in NLS0 and NLS7 are approximately 6–8%. It is unlikely that the higher amount of Fe^{3+} is due to oxidation of the NLS5 chloritoid during the isolation procedure, because the same procedure was used for all three cubes. As a result, all samples should show the same effect. No evidence for the presence of hematite (De Grave *et al.* 1984) or other iron oxides was found by Mössbauer spectroscopy or electron-microprobe analysis, also suggesting that the isolation procedure did not alter the chloritoid. The electron-microprobe analyses of chloritoid in pyrite also give similar results as those from the isolated grains of NLS5. Interestingly, the chloritoid in the (untreated) host rock of the pyrite has a similar $\text{Fe}^{3+}/\text{Fe}^{2+}$ value as chloritoid isolated from NLS5. This may indicate a bimodal distribution of $\text{Fe}^{3+}/\text{Fe}^{2+}$ in chloritoid from the pyrite-bearing locality.

When atomic proportions are normalized so that $\text{Si} = 2$, the sum of trivalent atoms ($\text{Al}^{3+} + \text{Fe}^{3+}$) is somewhat higher than four, and the sum of divalent cations ($\text{Mg}^{2+} + \text{Mn}^{2+} + \text{Fe}^{2+}$) is less than the expected

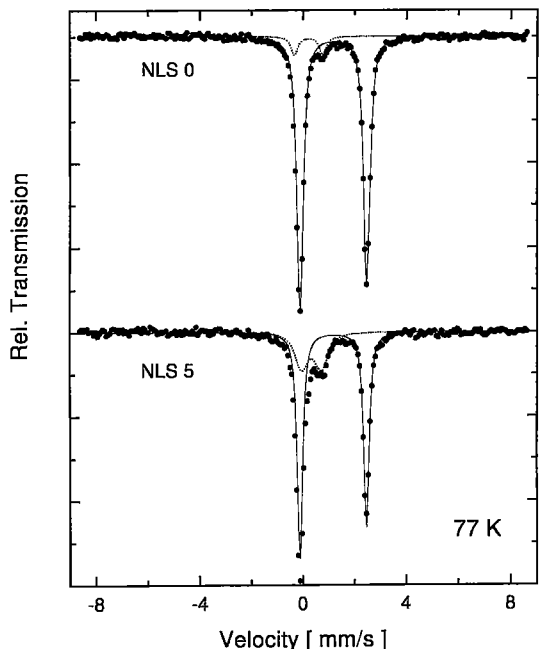


FIG. 4. Mössbauer spectra of samples NLS0 and NLS5 taken at 77 Kelvin. The full line corresponds to the Fe^{2+} component, and the dotted line, to Fe^{3+} , respectively.

TABLE 3. MÖSSBAUER PARAMETERS FOR CHLORITOID SAMPLES

Sample	Fe ²⁺			Fe ³⁺			Notes
	IS	EQ	Area	IS	EQ	Area	
NLS0	1.15	2.44	94.0	0.25	0.98	6.0	room temp.
	±0.03*	±0.04	±1.5	±0.02	±0.05	±1.5	
	1.28	2.58	93.0	0.32	1.10	7.0	77 K
	±0.04	±0.05	±2.0	±0.02	±0.04	±2.0	
NLS7	1.18	2.43	92.0	0.28	0.95	8.0	room temp.
	±0.03	±0.02	±3.0	±0.03	±0.04	±3.0	
NLS5	1.16	2.45	80.0	0.40	0.68	20.0	room temp.
	±0.03	±0.04	±3.0	±0.03	±0.06	±3.0	
	1.28	2.57	75.0	0.45	0.76	25.0	77 K
	±0.04	±0.05	±4.0	±0.03	±0.05	±4.0	

* The variances are estimated from different fits to the spectra.

from the data, possible hydration of the Fe²⁺ site may require further study.

Results of Mössbauer spectroscopy

The room-temperature (RT) Mössbauer spectra of samples NLS0, NLS5, and NLS7 are shown in Figures 3a and 3b, and the 77 Kelvin spectra of NLS0 and NLS5 are given in Figure 4. All spectra could be fit by two quadrupole-split doublets for the dominating Fe²⁺ component, which is consistent with the results of De Grave *et al.* (1984), indicating that Fe²⁺ is present in only one type of structural site.

Because of preferred orientation (texture) effects, asymmetric doublets had to be used for the analysis. The asymmetry in the spectrum was still present after grinding the samples to a very fine powder. The techniques proposed by Rancourt (1994) to remove the preferred orientation were unsuccessful. The presence of a texture effect and its influence on the Fe³⁺/Fe²⁺ value was verified by measurements taken at different

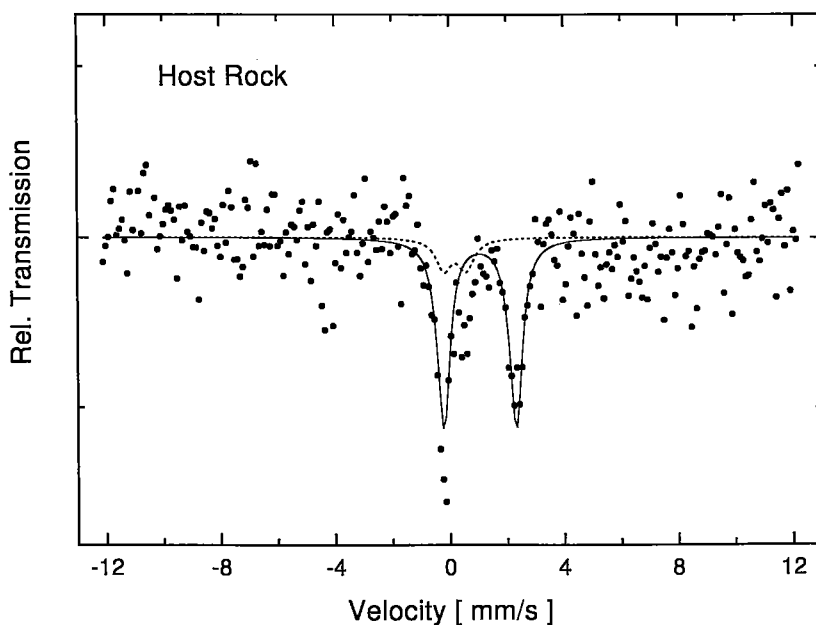


FIG. 5. Room-temperature Mössbauer spectrum of the host rock of the pyrite cubes.

value of two (see footnotes, Table 2). Note, however, that the sum of divalent and trivalent cations is about the expected value of six in any of the cubes. It appears that Fe³⁺ does not substitute for Al³⁺, as the general formula suggests, but that Fe³⁺ substitutes instead for Fe²⁺. The atomic proportions of 'OH' are also greater than the expected value of four. Although no clear relation between Fe³⁺ excess and OH excess is apparent

angles of incidence between the sample and the γ -ray direction. Spectra taken at an angle of $50 \pm 5^\circ$ (magic angle; see Fig. 3b) could be fit perfectly by two symmetric doublets, as expected in the case of texture present in the sample. In the ideal case, the linewidths of both spectra shown in Figure 3b should be the same. However, the linewidth in the 50° spectrum is broader than in the 0° spectrum, which is probably caused by

the higher signal:noise ratio in the 50° spectrum. Within error limits, the $\text{Fe}^{3+}/\text{Fe}^{2+}$ value determined from the 50° measurement is the same as in measurements taken at 0° for sample NLS5. We assume that this result is also valid for the other samples, and used the spectra taken at 0° angles for the determination of the ratio $\text{Fe}^{3+}/\text{Fe}^{2+}$.

The Mössbauer parameters ΔEQ (quadrupole splitting of the doublet) and IS (isomer or center shift) determined for the high-intensity component (Table 3) are consistent with Fe^{2+} in chloritoid as determined by Tricker *et al.* (1978), Hålenius *et al.* (1981), and De Grave *et al.* (1984). These values are typical for octahedral sites. In contrast to the results of De Grave *et al.* (1984), there was no need to use two Fe^{2+} doublets to fit the data.

The low-intensity component in samples NLS0 and NLS7 was assigned to Fe^{3+} , on the basis of its Mössbauer parameters (Table 3), which are very similar to the ones reported by Hålenius *et al.* (1981) and Tricker *et al.* (1978). The values of isomer shift, about +0.26 (± 0.02) mm/s at RT and +0.32 mm/s at 77 K, are slightly smaller than those reported in the literature [about +0.31 (± 0.02) and +0.40 (± 0.04), respectively]. However, the small difference can be easily explained by the complete overlap of the two low-velocity lines of Fe^{2+} and Fe^{3+} , which makes it difficult to determine the position of the Fe^{3+} resonance line very accurately. Indeed, the results of the fit for the different measurements show a larger scattering compared to the Fe^{2+} IS values.

The relative intensities of the Fe^{3+} component in the RT spectra for NLS0 and NLS7 were determined as about 6% and 8%, respectively, assuming that the *f*-factor is the same for the Fe^{2+} and the Fe^{3+} site. As pointed out by De Grave & Van Alboom (1991), this assumption could result in a slight overestimation of the Fe^{3+} content. This is probably not the case here, because the analysis of the 77 K spectrum for NLS0 gives a value of ~7%, which is very close to the RT result, and indicates that differences in the *f*-factors are small.

The situation is somewhat different for sample NLS5. A visual comparison of the spectra of NLS0, NLS7, and NLS5 (Figs. 3a, 4) shows that the intensity of the Fe^{3+} component is significantly higher in NLS5 than in NLS0 and NLS7. The analysis of different measurements from sample NLS5 yields relative Fe^{3+} intensity values of about 22.0 (± 3.0)% at both RT and 77 K, which is nearly a factor of three higher than those for NLS0 and NLS7.

In addition, the values for quadrupole splitting and isomer shift in NLS5 are different from those in NLS0 and NLS7, assuming that only one Fe^{3+} component is present (Table 3). Thus the different Mössbauer parameters suggest that Fe^{3+} in NLS5 chloritoid occupies different crystallographic sites than Fe^{3+} in chloritoid from cubes NLS0 and NLS7.

However, the total iron content and crystal structure (based on XRD analyses) of NLS5 chloritoid is similar to that in cubes NLS0 or NLS7. The common place of origin and probably similar conditions of formation of the pyrite samples leads us to expect at least one common Fe^{3+} site in all three samples of chloritoid. To test this concept, we have analyzed the NLS5 Mössbauer data using one Fe^{2+} component and two different Fe^{3+} components. The isomer shift and quadrupole splitting values of one of the two Fe^{3+} components were set to be equal to the Fe^{3+} values found in NLS0 and NLS7 chloritoid (assigned to $\text{Fe}^{3+}(\text{I})$ in the following).

Although the statistical quality of the fit for both the RT and 77 K spectra did not improve significantly using a three-component fit, the results yield relative intensities for the $\text{Fe}^{3+}(\text{I})$ component in NLS5 that are very similar to those in NLS0 or NLS7. The relative intensities of the $\text{Fe}^{3+}(\text{I})$ component are about 8% and 9% at RT and 77 K, respectively, whereas the relative intensities of the other Fe^{3+} component [$\text{Fe}^{3+}(\text{II})$] are 10% and 16%, respectively. The three-component fit thus gives a relative intensity for $\text{Fe}^{3+}(\text{I})$ closer to that expected from stoichiometry ($\text{Fe}^{3+} + \text{Al}^{3+} \approx 4$), as has been found for NLS0 and NLS7 (Table 2). The Mössbauer parameters of the $\text{Fe}^{3+}(\text{II})$ component are IS = 0.50 (± 0.04) mm/s, $\Delta\text{EQ} = 0.63$ (± 0.04) mm/s at RT, and IS = 0.56 (± 0.04) mm/s, $\Delta\text{EQ} = 0.60$ (± 0.04) mm/s at 77 K, respectively. The uncertainties in these values are due to the large overlap between the two Fe^{3+} components.

The excess of about 10% Fe^{3+} in NLS5 in the form of the $\text{Fe}^{3+}(\text{II})$ component may be explained by the presence of some oxidized Fe^{3+} in the structural sites normally occupied by Fe^{2+} . A simple picture of the chloritoid structure is given by two sheets of edge-sharing octahedra linked by isolated SiO_4 tetrahedra and OH bonds (for more details, see Tricker *et al.* 1978). One type of octahedral site is occupied by Al^{3+} and Fe^{3+} , whereas the second site is occupied by divalent cations (Mg^{2+} , Mn^{2+} , Fe^{2+}). It seems unlikely that the $\text{Fe}^{3+}(\text{II})$ component from NLS5 is located in the same layer containing Al^{3+} and $\text{Fe}^{3+}(\text{I})$, as mentioned above in the section on results of electron-microprobe analyses. The Mössbauer parameters of the $\text{Fe}^{3+}(\text{II})$ component suggest an octahedral coordination, which may be consistent with oxidation of Fe^{2+} to Fe^{3+} in the other layer of octahedra that normally host divalent cations in chloritoid.

Pyrite host-rock

A small amount of the pyrite host-rock was obtained and examined by electron microscopy, XRD analysis, and Mössbauer spectroscopy. The metamorphic host-rock exhibits a classic porphyroblastic texture. Large pods consisting predominantly of muscovite are included in a very fine-grained mixture of K-feldspar

and quartz. Common accessory minerals in the groundmass include chloritoid and rutile. X-ray-diffraction analysis of the host rock confirmed the presence of muscovite, quartz, and microcline. Minor amounts of chloritoid were also identified in the X-ray-diffraction pattern, but pyrite seems to be absent. The composition of chloritoid in the host rock is also listed in Table 2. This chloritoid is similar to that found in the pyrite cube NLS5, except for slightly higher Mg and Mn contents.

The Mössbauer spectrum of the host rock, given in Figure 5, shows an asymmetric doublet structure, which can be fit by two symmetric doublet components. The dominant component present in the host rock is Fe²⁺, which is attributed to chloritoid with similar Mössbauer parameters, as found for the isolated chloritoid (Table 3). However, the amount of chloritoid in the host rock is very minor, as indicated by the rather small signal-to-background ratio of about 10⁻³ for a sample thickness of about 40 mg/cm². The other component with an isomer shift of +0.30 (0.02) mm/s and a quadrupole splitting of 0.79 (0.03) mm/s is attributed to Fe³⁺, which probably belongs to the chloritoid because the parameters are the same as found for the Fe³⁺ in cube NLS5. The relative intensities, about 80% for Fe²⁺ and 20% for Fe³⁺, are also very similar to the ones determined for the chloritoid from cube NLS5 (see also Table 3). Fits to the Mössbauer spectrum are consistent with the absence of pyrite or other Fe-sulfides in the host rock, but because of the high signal-to-noise ratio, their presence in very small amounts cannot be ruled out. The X-ray-diffraction spectrum shows that the host rock mainly consists of muscovite, whereas the Mössbauer parameters indicate no evidence for muscovite, suggesting that the iron content of the muscovite must be very low.

CONCLUSIONS

We identified chloritoid close to the iron end-member as the major silicate inclusion in pyrite cubes from Navajún, Spain. Mössbauer spectroscopy and X-ray-diffraction analyses both show that the chloritoid exhibits preferred textural and orientation effects. The Fe³⁺ content of the chloritoid among different pyrite cubes is variable, and at least two populations, with total iron as Fe³⁺ of 6–8% and 22% are found. The Fe³⁺ does not seem to replace Al³⁺ in the crystal structure. It appears that Fe²⁺ was oxidized to Fe³⁺ in the layer of octahedra that normally host divalent cations in chloritoid.

ACKNOWLEDGEMENTS

We thank Bernhard Spettel for providing the INA analyses and Brad Jolliff for useful comments, which helped to improve the manuscript. We also thank Bruce Fegley for constructive comments. Of the two anonymous referees, we wish to thank the one who made useful suggestions regarding the Mössbauer data. Work supported by NASA grant NAGW-2867 and NATO collaborative research grant 931476.

REFERENCES

- ARMSTRONG, J.T. (1988): Quantitative analysis of silicate and oxide minerals: comparison of Monte-Carlo, ZAF, and Phi-Rho-Z procedures. *Microbeam Anal.* **23**, 239-246.
- CALVO, M. & SEVILLANO, E. (1989): Pyrite crystals from Soria and La Rioja provinces Spain. *Mineral. Rec.* **20**, 451-456.
- CHOPIN, C., SEIDEL, E., THEYE, T., FERRARIS, G., IVALDI, G. & CATTI, M. (1992): Magnesiochloritoid, and the Fe-Mg series in the chloritoid group. *Eur. J. Mineral.* **4**, 67-76.
- DEER, W.A., HOWE, R.A. & ZUSSMAN, J. (1966): *An Introduction to the Rock-Forming Minerals*. Longman, London, U.K.
- DE GRAVE, E. & VAN ALBOOM, A. (1991): Evaluation of ferrous and ferric Mössbauer fractions. *Phys. Chem. Minerals* **18**, 337-342.
- _____, VANLEERBERGHE, R., VERDONCK, L. & DE GEYTER, G. (1984): Mössbauer and infrared spectroscopic studies of Belgian chloritoids. *Phys. Chem. Minerals* **11**, 85-94.
- FEGLEY, B., LODDERS, K., TREIMAN, A. H. & KLINGELHÖFER, G. (1995): The rate of pyrite decomposition on the surface of Venus. *Icarus* **115**, 159-180.
- GUSTAFSON, J.K. (1946): Two occurrences of chloritoid as a hydrothermal mineral in igneous rocks. *Am. Mineral.* **31**, 313-316.
- HÄLENIUS, U., ANNERSTEN, H. & LANGER, K. (1981): Spectroscopic studies on natural chloritoids. *Phys. Chem. Minerals* **7**, 117-123.
- HALFERDAHL, L.B. (1961), Chloritoid: its composition, X-ray and optical properties, stability, and occurrence. *J. Petrol.* **2**, 49-135.
- KLINGELHÖFER, G., HELD, P., TEUCHER, R., SCHLICHTING, F., FOH, J. & KANKLEIT, E. (1995): Mössbauer spectroscopy in space. *Hyperfine Interactions* **95**, 305-339.
- RANCOURT, D.G. (1994): Mössbauer spectroscopy of minerals. I. Inadequacy of Lorentzian-line doublets in fitting spectra arising from quadrupole splitting distributions. *Phys. Chem. Minerals* **21**, 244-249.
- TRICKER, M.J., JEFFERSON, D.A., THOMAS, J.M., MANNING, P.G. & ELLIOTT, C.J. (1978): Mössbauer and analytical electron microscopic studies of an unusual orthosilicate: chloritoid. *J. Chem. Soc., Farad. Trans.* **2**, **74**, 174-181.
- VIDAL, O., THEYE, T. & CHOPIN, C. (1994): Experimental study of chloritoid stability at high pressure and various fO₂ conditions. *Contrib. Mineral. Petrol.* **118**, 256-270.

Received March 20, 1997, revised manuscript accepted November 10, 1997.